

# EXPERIMENTAL VERIFICATION OF MATHEMATICAL MODELS FOR TIRE-SOIL INTERACTION

Siwakorn Phakdee<sup>1,3</sup>, Juthanee Phromjan<sup>1,3</sup>, Ravivat Rugsaj<sup>2</sup> and Chakrit Suvanjumrat<sup>1,3\*</sup>

<sup>1</sup>Department of Mechanical Engineering, Faculty of Engineering, Mahidol University, Salaya, Nakhon Pathom 73170, Thailand;

<sup>2</sup>Department of Mechatronics Engineering and Artificial Intelligence, Vincent Mary School of Engineering, Assumption University, Samut Prakan 10570, Thailand;

<sup>3</sup>Laboratory of Computer Mechanics for Design (LCMD), Department of Mechanical Engineering, Faculty of Engineering, Mahidol University, Salaya, Nakhon Pathom 73170, Thailand

\*Corresponding Author, Received: 06 Aug. 2023, Revised: 12 Dec. 2023, Accepted: 15 Dec. 2023

**ABSTRACT:** This study delves into an in-depth exploration of tractor tire performance on soft ground, with a specific focus on the intricate relationships between shear stress, slip displacement, and net traction. Leveraging a meticulously designed Tire Testing Machine (TTM) tailored for laboratory-scale analyses, the study systematically investigates three distinct tread depths of tractor tires. The TTM's unique capability to exert precise control over environmental conditions during tire compression and rolling on a designated soil surface underscores the methodological rigor of the investigation. Throughout the study, rigorous measurements of traction force, compression load, and vertical displacement were conducted to rigorously validate pressure-sinkage and net traction equations. A thorough analysis illuminates inherent errors and limitations within prevailing prediction models, providing a critical foundation for the refinement of future equations. The acquired experimental data not only offer indispensable insights guiding the development of more accurate predictive models but also establish a benchmark for the validation of finite element models in subsequent research endeavors. This work significantly contributes to the nuanced understanding of tire dynamics on soft ground, emphasizing the pivotal role of the TTM in ensuring a controlled environment for obtaining reliable experimental data. The delineated findings and limitations not only enrich the engineering discourse but also set the stage for ongoing research endeavors aimed at advancing predictive models and elevating our understanding of tire dynamics in the context of agricultural machinery navigating challenging terrains.

*Keywords: Agriculture, Single-wheel tester, Tractive force, Tractor tire*

## 1. INTRODUCTION

Thailand stands out as a major player in sugarcane production within Southeast Asia [1], securing the fourth spot globally [2]. Consequently, the adoption of tractors in Thailand has been steadily increasing over the years. Tractors play a pivotal role in reducing time and labor costs in farming [3], particularly when equipped with cultivators for essential agricultural processes like tilling, sowing, and harvesting. The tractor tires are critical components that come into direct contact with and impact the soil during agricultural operations. From this perspective, the efficiency of tire traction is a key focus of this study, as it directly influences fuel consumption and productivity [4]. Numerous researchers have delved into the study of tire traction efficiency using a combination of experimental and semi-empirical methods [5]. For instance, Shafaei et al. [6] meticulously recorded agricultural processes and tractor tractive efficiency to train the adaptive neuro-fuzzy inference system. Many of these studies have involved experiments ranging from laboratory-scale indoor single-wheel testers to full-field scale setups [7]. The Universiti Putra Malaysia tire traction testing

facility, developed by [8], has been instrumental in studying high-lug agricultural tire traction. This facility is capable of measuring traction force, tire sinkage, and traveling speed during tests, with all measurement data being recorded in real-time by the data acquisition system. Farhadi et al. [9] employed 3D-scanning techniques to explore the impact of tractor tire contact volume on rolling resistance using an indoor single-wheel tester. Phakdee and Suvanjumrat [10] developed the tire testing machine (TTM) to study tire-soil interaction on a laboratory scale. The TTM, used in conjunction with the 3D scanning technique, measured and illustrated the soil bulk density of 3D tractor tire footprint models as a color contour. Phromjan and Suvanjumrat [11] used the TTM to study nonpneumatic tires (NPTs) for agriculture. In this study, the NPT, reduced-spoke NPT, and pneumatic tire were utilized to perform compression testing. The soil compaction effect from these three tires was compared and discussed in this study. In the realm of semi-empirical methods, Bekker [12] developed and proposed the pressure-sinkage equation, derived from two plate penetration testing, capable of predicting soil sinkage. Additionally, Bekker formulated the motion

resistance equation, derived from the pressure-sinkage equation, to quantify the energy expended during soil compaction. This equation enables the prediction of net traction, calculated as the difference between gross tractive force and motion resistance. Bekker's equations are applicable in both rigid and elastic tire modes [5, 13, 14]. Several researchers modified and verified the Bekker equation through experimental methods. Pan et al. [15] modified and developed the pressure-sinkage equation by incorporating additional parameters such as soil water content, bulk density, and slope angle. In a similar vein, Meirion-Griffith and Spenko [16] modified the pressure-sinkage equation to become suitable for tires with diameters less than 50 cm and then verified it with Bekker's equation. However, it's noteworthy that the verification of the Bekker equation has been primarily limited to rigid tire mode conditions due to challenges in controlling testing conditions and parameters.

## 2. RESEARCH SIGNIFICANCE

The primary objective of this research was to verify Bekker's equations with the experimental data, specifically focusing on parameters such as maximum soil sinkage and net traction under conditions of elastic-mode tires. These experiments were conducted on a laboratory scale employing TTM. The outcomes of this study serve not only as a strategy but also as a guideline for refining and enhancing Bekker's equations. Additionally, the experimental data generated can prove invaluable for validating finite element models in future research endeavors.

## 3. THEORIES

The pressure-sinkage equation, as expressed in Eq. (1), is grounded in the correlation between the contact pressure ( $\bar{q}_z$ ) and the soil sinkage ( $z$ ).

$$\bar{q}_z = (k_c / b + k_\phi) z^n, \quad (1)$$

where  $k_c$  and  $k_\phi$  denote the soil parameters and  $n$  denotes the model constant.  $k_c$ ,  $k_\phi$ , and  $n$  can be obtained from the two plates penetration in pressure-sinkage testing, and  $b$  denotes the shorter length of the contact shape.

The net traction ( $NT$ ) for a tire operating in the elastic tire mode is defined as the difference between the gross tractive force ( $GT$ ) and the motion resistance ( $R_c$ ), as outlined in Eq. (2).

$$NT = GT - R_c. \quad (2)$$

In accordance with references [5, 17], the tire traction diagram under the elastic mode is illustrated

in Fig. 1. The gross tractive force can be precisely defined by Eq. (3).

$$GT = br \left[ \int_{\theta_c}^{\theta_1} \tau(\theta) \cos \theta d\theta + \frac{1}{r} \int_0^{l_{AB}} \tau(x) dx + \int_{\theta_2}^{\theta_c} \{ \tau(\theta) \cos \theta - \sigma(\theta) \sin \theta \} d\theta \right], \quad (3)$$

where  $\theta_1$  and  $\theta_2$  denote the contact angle at the leading and trailing edge of the tire-soil interface, and  $l_{AB}$  denotes the length of the contact area can be calculated from  $l_{AB} = 2r \cos \theta_c$ . The normal stress ( $\sigma(\theta)$ ) can be computed as a function of pressure-sinkage utilizing Eq. (1).

The shear stress ( $\tau(\theta)$ ) can be defined by

$$\tau(\theta) = \{ c + \sigma(\theta) \tan \phi \} \left[ 1 - \exp \left\{ -r/k \{ (\theta_1 - \theta) - (1-s)(\sin \theta_1 - \sin \theta) \} \right\} \right], \quad (4)$$

where  $c$  denotes the cohesion,  $\phi$  denotes the internal friction angle, and  $k$  denotes the compressive property of soil.

The motion resistance can be obtained by

$$R_c = br \int_{\theta_c}^{\theta_1} \sigma(\theta) \sin \theta d\theta. \quad (5)$$

Substituting Eqs. (3), (4), and (5) into Eq. (2). Thus, the net traction ( $NT$ ) can be obtained from

$$NT = \left[ br \left[ (c\theta - \sigma \tan \phi \theta) - \left[ k / (r(1-s)) * (\sin \theta_1 - \sin \theta) \right] \right] * e^M \Big|_{\theta_c}^{\theta_1} + \frac{F/A}{r} x \Big|_0^{l_{AB}} + (c\theta - \sigma \tan \phi \theta) - \left[ -k / (r(1-s)) (\sin \theta_1 - \sin \theta) \right] * e^M \Big|_{\theta_2}^{\theta_c} \right] + br \frac{F}{A} \cos \theta \Big|_{\theta_c}^{\theta_1}, \quad (6)$$

where  $M = -r/k(\theta_1 - \theta - (1-s)(\sin \theta_1 - \sin \theta))$ .

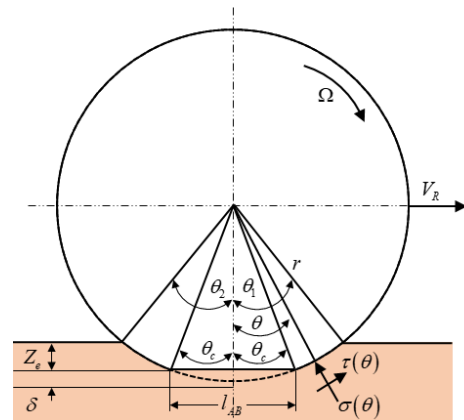


Fig. 1 Tire traction diagram in the elastic mode.

## 4. MATERIALS AND METHODS

### 4.1 Soil Testing

The soil for testing was obtained from the sugarcane cultivation area in Nakhon Pathom province, Thailand. The sampled soil was identified as sandy clay loam soil, and its particle distribution was determined through sieve and hydrometer analysis in accordance with the ASTM D422-63 Standard, Test Method for Particle-Size Analysis of Soils. The analysis revealed a composition of 60% sand, 13% silt, and 23% clay in the soil.

Isotropically consolidated undrained triaxial compression tests were conducted to determine the shear strength parameters of the tested soil. The results indicated that the testing soil possessed an internal friction angle ( $\phi$ ) of  $19.8^\circ$  and a cohesion ( $c$ ) of 11.174 kPa. Additionally, the compressive property of the soil ( $k$ ) was obtained from the literature review [18], which featured comparable soil properties.

The initial conditions of the testing soil comprised a dry bulk density of  $1.5 \text{ Mg/m}^3$  and a moisture content of 15% w/w. These conditions were deemed suitable for cultivation, as referenced in [18].

### 4.2 Tire Testing Machine

The TTM consists of two primary components: the soil bin and the single-wheel tester, both affixed to the TTM structure, as depicted in Fig. 2. The soil bin, measuring 150 cm in width, 300 cm in length, and 85 cm in height, served for soil preparation, simulating agricultural soil conditions without interference from the soil bin wall boundary. The single-wheel tester conducted both tire compression and traction tests. Utilizing a hydraulic cylinder, the TTM could compress agricultural tires under specified vertical load and displacement conditions. The hydraulic cylinder ensured precision in applied vertical load and displacement, with tolerances of  $\pm 1 \text{ N}$  and  $\pm 1 \text{ mm}$ , respectively.



Fig. 2 The developed tire testing machine.

The single-wheel tester could move smoothly along the structure base via rollers with minimal friction, powered by an electric winch mounted at the structure base. Experimental data, encompassing loads and displacement, were collected in real-time through the TTM's measurement devices (S-beam load cells and Linear displacement sensor) at a sampling rate of 5 Hz via the data acquisition system. The reported accuracy of the load cells and linear displacement sensor stood at 6.92% and 4.74%, respectively.

### 4.3 Pressure-Sinkage Testing

The soil parameters ( $k_c$  and  $k_\phi$ ), along with the constant ( $n$ ), represent the unknowns in the pressure-sinkage equation, and their determination involved pressure-sinkage testing. This testing method employed two cylindrical plungers, each with diameters of 14 cm and 22 cm (see Fig. 3). These plungers were installed in the single-wheel tester at the mounting jig and compressed against the testing soil in the soil bin, as illustrated in Fig. 4. The vertical displacement conditions for plunger compression in the pressure-sinkage test varied from 1 cm to 4 cm with an interval of 1 cm. This approach allowed for a systematic exploration of the relationship between pressure and sinkage under different conditions, enabling the precise determination of the unknown parameters in the pressure-sinkage equation.



Fig. 3 Two different sizes of the cylindrical plunger.

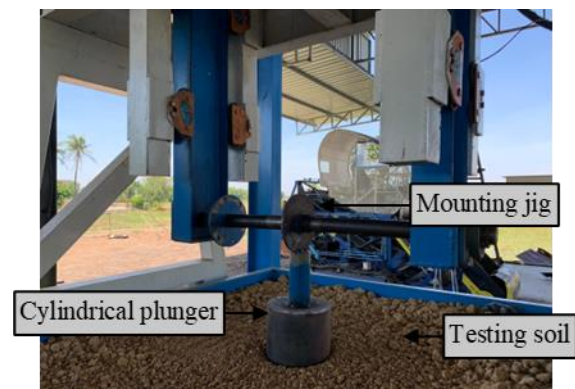


Fig. 4 Cylindrical plunger mounting on the TTM.

#### 4.4 Tire Testing

The dimensions of the agricultural tire employed in the experiment are depicted in Fig. 5, and its key characteristics are summarized in Table 1. The agricultural tires, labeled as tractor tires A, B, and C, showcase varying tread depths. Thorough compression and traction tests were performed on these tires utilizing the TTM. This testing procedure allowed for a comprehensive evaluation of the performance characteristics of each tire, providing valuable insights into their behavior under different conditions.

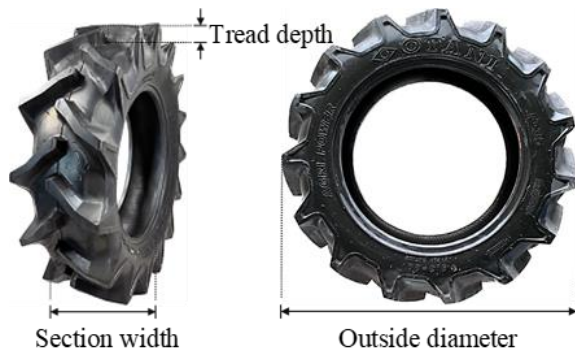


Fig. 5 The agricultural tire dimensions.

Table 1 Tractor tire specification

Tractor tires	size	Outside diameter (mm)	Section width (mm)	Tread depth (mm)
A	8.3-20	890	208	30
B	8.3-20	890	215	36
C	8.3-20	890	200	44.45

In the compression test, the tractor tire was secured to the single-wheel tester at the mounting jig, as shown in Fig. 6. The hydraulic cylinder applied compression to the tire against the soil, subject to a specified vertical load condition. This load condition encompassed the combined weight of the tractor, fuel, equipment, and driver, representing the usage load for a light-segment tractor, as detailed in Table 2. It's noteworthy that the total tractor usage load was distributed among the tires, with a safety factor of 2. Consequently, the compression test was conducted under a vertical load of 4,750 N, ensuring a robust testing condition that mimics realistic operational scenarios.

Throughout this process, the vertical load and displacement were monitored using the vertical S-beam load cell positioned at the hydraulic cylinder and the vertical linear displacement sensor, respectively, as illustrated in Fig. 7. These measurement devices provided accurate and real-time data, enabling precise assessment of the tire's response to the applied compression force and

vertical displacement. The integration of such instrumentation contributes to the reliability and comprehensiveness of the compression test results, facilitating a thorough understanding of the tire's behavior under specified conditions.

In the traction test, the agricultural tires experienced compression against the soil under a consistent vertical load condition of 4,750 N, mirroring the procedure of the compression test. Subsequently, the tires were subjected to traction by an electric winch. The traction test was conducted immediately after the compression test. The electric winch facilitated the movement of the agricultural tire, along with the single-wheel tester, across the soil surface for a distance of 1.12 m at a constant velocity of 0.02 m/s. This systematic approach allowed for the evaluation of the tire's traction performance, providing insights into its ability to maintain traction and resist slippage under controlled conditions.



Fig. 6 Tractor tire mounting on the TTM.

Table 2 The usage loads of light-segment tractor

Lists	Weight (kg)
Tractor	650
Fuel	20
Equipment	210
Driver	70

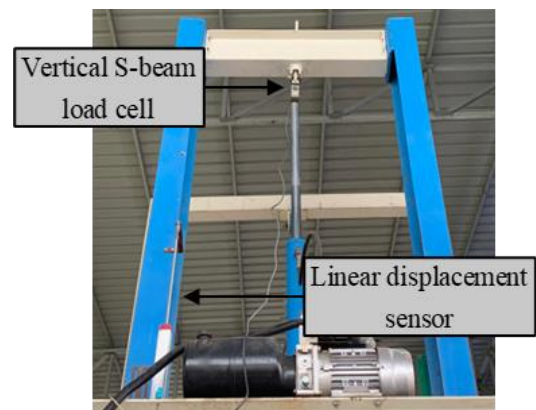


Fig. 7 Vertical load and displacement measurement devices

It is crucial to emphasize that the traction test was carried out under conditions indicative of low slip, a characteristic pertinent to tractor tires. Throughout this test, both the vertical load and displacement were monitored using the vertical S-beam load cell and the linear displacement sensor, respectively. Simultaneously, the traction force was measured using the horizontal S-beam load cell located at the wire rope sling of the electric winch, as illustrated in Fig. 8. This meticulous measurement setup ensured a comprehensive assessment of the tire's performance under controlled traction conditions, allowing for a nuanced understanding of its ability to maintain traction without excessive slippage.

After the conclusion of both compression and traction testing, the footprints left by the tractor tires on the soil surface were scanned using a portable 3D scanner, depicted in Fig. 9. This scanner boasts a resolution and accuracy of 50 and 30  $\mu\text{m}$ , respectively. The resulting 3D models of the tractor tire footprints hold significant utility for the analysis of soil sinkage and the determination of the contact area of the tractor tires. Leveraging these detailed 3D models allows for a thorough examination of the imprint left by the tires, offering insights into the interaction between the tires and the soil during both the compression and traction phases of testing.

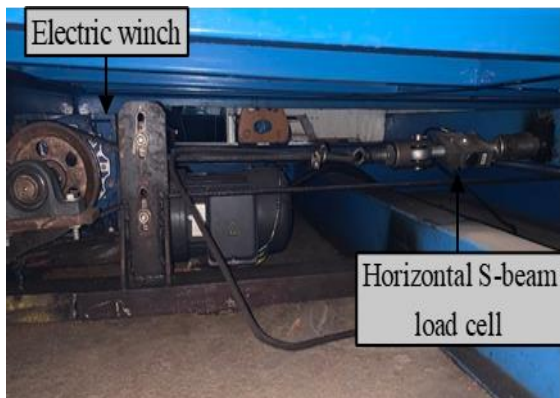


Fig. 8 Traction force measurement device



Fig. 9 3D scanning of the tractor tire footprint

## 5. RESULTS AND DISCUSSIONS

### 5.1 Pressure-Sinkage Equation

From the pressure-sinkage testing, the obtained data of soil sinkage, vertical load, and contact pressure were utilized to determine the variables of the pressure-sinkage equation. Consequently, the values for  $k_c$ ,  $k_\phi$ , and  $n$  were determined as  $k_c = 2,121,889$ ,  $k_\phi = -2,830.991$ , and  $n = 0.93$ . Substituting these variables into Eq. (1), the pressure-sinkage equation can be expressed as follows:

$$\bar{q}_z = (2,121,889 / (b - 2,830.991)) z^{0.93}, \quad (7)$$

where  $\bar{q}_z$  denotes the contact pressure,  $z$  denotes the soil sinkage, and  $b$  denotes the shorter length of the contact shape.

### 5.2 Tire Compression and Traction Testing

The 3D models generated from the compression and traction tests on agricultural tire footprints were utilized for soil sinkage depth analysis through CAD software. Soil sinkage, defined as the distance from the soil surface to the lowest point of the contact interface [19], was examined by projecting the side view of the 3D models, as shown in Fig. 10. The deformation of the tire was quantified by calculating the difference between the vertical displacement and soil sinkage. Additionally, the 3D sinkage model was visually represented as a color contour indicating depth using MATLAB software, as depicted in Fig. 11. This methodology provided a detailed and visual understanding of the soil sinkage patterns resulting from the tractor tire interactions, facilitating a comprehensive analysis of the tire's impact on the soil during both compression and traction phases.

This model serves to delineate the contact area of the agricultural tire by marking the boundary of contact area footprints with a blue line at a soil sinkage depth exceeding 21 mm, as indicated by the tire traction diagram (Fig. 1). It's important to highlight that, according to the study by Phromjan and Suvanjumrat [20-22], the contact area for compaction testing is deemed equivalent to that of traction testing. They reported that the contact path characteristics of a compressed tire on a flat surface were similar and capable of representing the contact path of a rolling tire. This alignment underscores the significance of the obtained contact area data, emphasizing its relevance for both compaction and traction scenarios in the agricultural tire testing context.

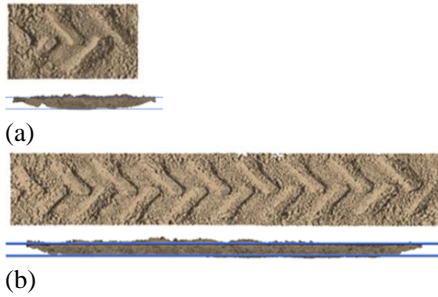


Fig. 10 3D soil sinkage model of (a) compression testing, and (b) traction testing.

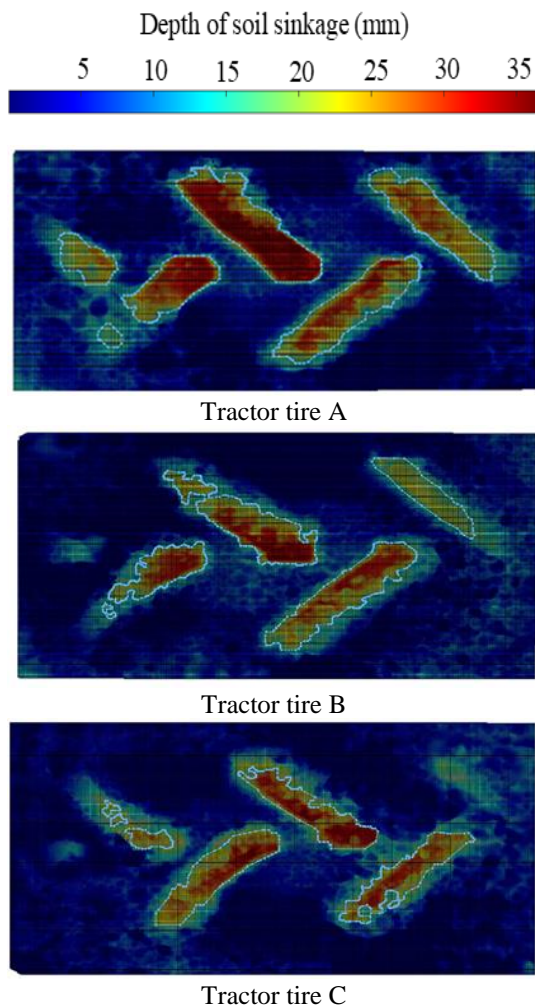


Fig. 11 Contact area analysis of the tractor tires.

The outcomes derived from the measurement of vertical load cell, horizontal load cell, and linear displacement sensor during both compression and traction tests, combined with the analysis of 3D agricultural tire sinkage models encapsulating soil sinkage and contact area analyses, are summarized in Tables 3 and 4, respectively. These tables provide a comprehensive overview of the gathered data, offering insights into the displacement, forces, and corresponding analyses for a detailed understanding

of the tractor tire performance under the specified testing conditions.

Table 3 The displacement results

Tractor tires	Vertical displacement (mm)	Soil sinkage (mm)	Tire deformation (mm)
A	48.15	34	14.15
B	48.9	36	12.9
C	53	40	13

Table 4 The action forces results

Tractor tires	Vertical load (N)	Contact area (m <sup>2</sup> )	Contact Pressure (kPa)	Traction force (N)
A	5,030	0.0265	190.130	1,266.90
B	4,892	0.0262	186.532	1,133.75
C	5,000	0.0220	227.331	1,109.02

### 5.3 Verification of Tire-Soil Interaction Equations

#### 5.3.1 Pressure-sinkage equation

The pressure-sinkage equation derived from the pressure-sinkage testing (Eq. 7) was validated using experimental results obtained from the compression testing (refer to Table 3). The variables' values acquired through experimentation were substituted into Eq. 7, and the soil sinkage results from the pressure-sinkage equation were compared with the experimental results, as outlined in Table 5. The equation demonstrated mean soil sinkage errors of 3.09%, 5.78%, and 5.80% for agricultural tires A, B, and C, respectively. These comparison results were visually represented in Fig. 12, where the experimental sinkage results were graphically compared with the predicted values, revealing a correlation coefficient ( $R^2$ ) of 0.981. Both the experimental and predicted outcomes exhibited satisfactory agreement.

It's worth noting that the agricultural tire with a smaller contact area exhibited deeper soil sinkage compared to the larger ones. This observation aligns with the findings of Smith and Dickson [23], who reported that the depth of soil sinkage increases proportionally with the increasing ground pressure. Consequently, under identical vertical load conditions, agricultural tire C, with the smallest contact area, generated the highest contact pressure and the deepest soil sinkage. In contrast, agricultural tires B and A, with larger contact areas, produced lower contact pressure, resulting in shallower soil sinkage.

Table 5 Comparison of soil sinkage results

Tractor tires	Soil sinkage (mm)		Error (%)
	Experiment	Prediction	
A	34	32.95	3.09
B	36	33.92	5.78
C	40	37.68	5.80

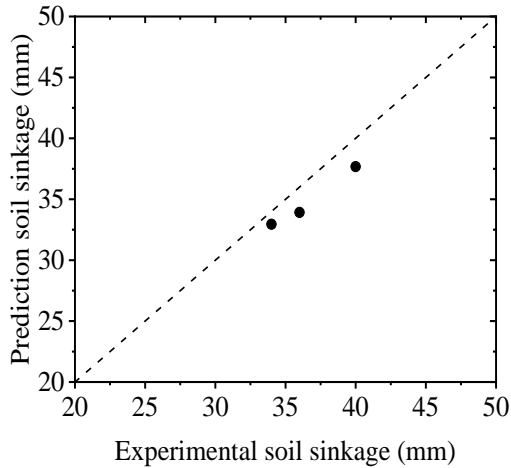


Fig. 12 Soil sinkage results of the experiment and the pressure-sinkage equation

5.3.2 Net traction equation

The verification of the net traction equation (Eq. 6) was carried out using experimental results from the traction test, akin to the process for verifying the pressure-sinkage equation. Variable values extracted from Tables 2 and 3 were substituted into Eq. 6, and the comparison between traction force results from the experiment and the predicted equation is presented in Table 6. The predicted results exhibited a trend that aligned well with the experimental outcomes, in line with the findings of ten Damme et al. [24], who reported that tires with higher contact areas would generate higher traction forces than those with lower contact areas.

However, it's noteworthy that the net traction equation tended to predict higher traction forces than observed in the experiment. This discrepancy can be attributed to the equation's limitation in predicting the net traction of elastic tires under the assumption of a smooth tread condition. This leads to an overestimation of the net traction force for agricultural tires with assumed smooth tread patterns compared to the actual net traction force measured in experiments with real tread patterns. This overestimation is consistent with the findings of Zeng et al. [25], who noted that, under low-slip conditions, smooth tires produced higher traction forces than tires with tread patterns due to the larger contact area generated by smooth tires.

Consequently, the net traction equation (Eq. 6) was modified by dividing it by 3.5. The calculated results from the modified equation demonstrated a satisfactory average error of 10.13%. Additionally, it's important to acknowledge that environmental factors, such as clods and rocks on the prepared soil surface, could contribute to errors in the results. These factors should be considered when interpreting and generalizing the findings of the net traction equation.

Table 6 Comparison of traction force results

Tractor tires	Traction force (N)		
	Experiment	Prediction	
		Original	Modified
A	1,266.90	5,227.47	1,004.79
B	1,133.75	3,844.66	1,493.56
C	1,109.02	3,516.77	1,098.47

6. CONCLUSION

The developed TTM proved valuable for studying tire-soil interaction under diverse conditions. Using three agricultural tires (8.3-20) with varying tread depths, compaction, and traction tests were conducted, measuring parameters like vertical load and displacement. Results, including soil sinkage and net traction, were validated using pressure-sinkage and net traction equations. The study demonstrated a favorable agreement (less than 4.89% error) between experimentally obtained soil sinkage and the pressure-sinkage equation. Disparities in net traction results were attributed to environmental conditions and limitations in the net traction equation designed for slick tires, emphasizing the need for tailored equations for lug treaded agricultural tires. The findings offer valuable insights for refining net traction equations and serve as a benchmark for validating Finite Element Method outcomes in future tire-soil interaction studies.

7. ACKNOWLEDGMENTS

This research, supported by Mahidol University's Laboratory of Computer Mechanics for Design, enabled the development of a tire testing machine and an in-depth study of tire-soil interaction. LCMD's collaboration was instrumental in achieving valuable insights for the research.

8. REFERENCES

- [1] OAE (Office of Agricultural Economics), ASEAN Agricultural Commodity Outlook No. 29 December 2022, Ministry of agricultural and cooperatives, 2022, pp. 1-87.
- [2] USDA (United States Department of Agriculture), 2018, Sugar : world markets and trade. <https://apps.fas.usda.gov/psdonline/circulars/sugar.pdf>. (Accessed 7 April 2023).
- [3] Wang X., Yamauchi F., and Huang J., Rising wages, mechanization, and the substitution between capital and labor: evidence from small scale farm system in China. *Agricultural Economics*, Vol. 47, 2016, pp. 309-317.
- [4] He R., Sandu C., Shenvi M. N., Mousavi H., Carrillo J., and Osorio J. E., Laboratory

- experimental study of tire tractive performance on soft soil: towing mode, traction mode, and multi-pass effect. *Journal of Terramechanics*, Vol. 95, 2021, pp. 33-58.
- [5] Nakajima Y., *Advance tire mechanics*, Springer, 2019, pp. 1-1245.
- [6] Shafael S.M., Loghavi M., and Kamgar S., An extensive validation of computer simulation frameworks for neural prognostication of tractor tractive efficiency. *Computers and Electronics in Agriculture*, Vol. 155, 2018, pp. 283-297.
- [7] Ozoemena A.A., Uzoejinwa B.B., Ezeama A.O., Onwualu A.P., Ugwu S.N., and Ohagwu C.J., Overview of soil-machine interaction studies in soil bin. *Soil and Tillage Research*, Vol. 175, 2018, pp. 13-27.
- [8] Yahya A., Zohadie M., Ahmad D., Elwaleed A.K., and Kheiralla A.F., UPM indoor tyre traction testing facility. *Journal of Terramechanics*, Vol. 44, 2007, pp. 293-301.
- [9] Farhadi P., Golmohammadi A., Sharifi A., and Shahgholi G., Potential of three-dimensional footprint mold in investigating the effect of tractor tire contact volume changes on rolling resistance. *Journal of Terramechanics*, Vol. 78, 2018, pp. 63-72.
- [10] Phakdee S. and Suvanjumrat C., Development of a tire testing machine for evaluating the performance of tractor tires based on the soil compaction, *Journal of Terramechanics*, Vol. 110, 2023, pp. 13-25.
- [11] Phromjan J. and Suvanjumrat C., Non-pneumatic tire with curved isolated spokes for agricultural machinery in agricultural fields: Empirical and numerical study, *Heliyon*, Vol. 9, Issue 8, 2023, pp. e18984.
- [12] Bekker M.G., *Introduction to Terrain-Vehicle Systems*, University of Michigan Press, 1969, pp. 1-846.
- [13] Wong J.Y., *Theory of Ground Vehicles*, John Wiley & Sons, Inc, 2001, pp. 1-523.
- [14] Wong J.Y., Chapter 4 - Characterization of the Response of Terrains to Normal and Repetitive Loadings, in: *Terramechanics and Off-Road Vehicle Engineering*. Elsevier, 2009, pp. 75-112.
- [15] Pan G., Sun J., Wang X., Yang F., and Liu Z., Construction and Experimental Verification of Sloped Terrain Soil Pressure-Sinkage Model. *Agriculture*, Vol. 243, 2021, pp. 1-17.
- [16] Meirion-Griffith G., and Spenko M., A modified pressure-sinkage model for small, rigid wheels on deformable terrains. *Journal of Terramechanics*, Vol. 48, 2011, pp. 149-155.
- [17] Muro T., and O'Brien J., *Terramechanics Land Locomotion Mechanics*, Swets & Zeitlinger B.V., 2005, pp. 1-273.
- [18] Mukhopadhyay S., Mastro R. E., Tripathi R. C., and Srivastava N. K., Chapter 14 – Application of Soil Quality Indicators for the Phytoremediation of Mine Spoil Dumps, in: *Phytomanagement of Polluted Sites*. Elsevier, 2019, pp. 361-388.
- [19] He R., Sandu C., Mousavi H., Shenvi M.N., Brun K., Kruger R., and Schalk Els P., Updated standards of the international society for Terrain-Vehicle Systems, *Journal of Terramechanics*, Vol. 91, 2020, pp. 185-231.
- [20] Phromjan J. and Suvanjumrat C., The contact patch characterization of various solid tire testing methods by finite element analysis and experiment. *Journal of Geomate*, Vol. 19, 2019, pp. 25-32.
- [21] Phromjan J. and Suvanjumrat C., Development of solid tire model for finite element analysis of compressive loading. *Songklanakarin Journal of Science and Technology*, Vol. 43, Issue 1, 2021, pp. 229-236.
- [22] Phromjan J. and Suvanjumrat C., Effects on spoke structure of non-pneumatic tires by finite element analysis. *International Journal of Automotive Technology*, Vol. 23, Issue 5, 2022, pp. 1437-1450.
- [23] Smith D.L.O., and Dickson J.W., Contributions of vehicle weight and ground pressure to soil compaction. *Journal of Agricultural Engineering Research*, Vol. 46, 1990, pp. 13-29.
- [24] ten Damme L., Schjønning P., Munkholm L.J., Green O., Nielsen S.K., and Lamandé M., Traction and repeated wheeling – effects on contact area characteristics and stresses in the upper subsoil. *Soil and Tillage Research*, Vol. 213, 2021, pp. 1-10.
- [25] Zeng H., Xu W., and Zang M., Experimental investigation of tire traction performance on granular terrain. *Journal of Terramechanics*, Vol. 104, 2022, pp. 49-58.
- 
- Copyright © Int. J. of GEOMATE All rights reserved, including making copies, unless permission is obtained from the copyright proprietors.